Subandean thrust and fold belt of northwestern Argentina: Geometry and timing of the Andean evolution

L. Echavarria, R. Hernández, R. Allmendinger, and J. Reynolds

ABSTRACT

The Subandean ranges of northwestern Argentina are an active thin-skinned fold and thrust belt. The main detachment level in Silurian shales dips 2–3°W, and all the major east-verging faults detach from it. Important intermediate detachment levels in the Devonian shales generate lift-off structures and the decoupling of the lower and upper structural levels. The Subandean thrust belt has a minimum shortening of about 60 km (36%) at about 22°40′ latitude. The deformation started at about 8.5–9 Ma with the uplift of the El Pescado range and the formation of an important back thrust at the Cinco Picachos range. Fault generation gets young to the east; the Pintascayo range uplift started at 7.6 Ma, while the Baja Orán range uplift began at about 6.9 Ma. These two ranges continued growing simultaneously until at least 4.7 Ma. At San Antonio range, fault movement began at approximately 4.4 Ma, and the Aguaragüe uplift started at about 2.7 Ma. An important stage dominated by out-of-sequence movements spans from about 4.5 Ma to present. For both proposed models of shortening, the Quaternary rates of shortening between 8 and 11 mm/yr coincide well with global positioning system results from the area. The hydrocarbon generation and migration is contemporaneous with the deformation, enhancing the possibilities of hydrocarbon entrapment in the area.

INTRODUCTION

The Subandean belt marks the eastern limit of the central Andes from Peru to northern Argentina (Figure 1). The belt is one of the only modern, active examples of a thin-skinned fold and thrust belt in a retroarc, noncollisional setting. As such, it is ideal for comparison with ancient retroarc belts such as the Cordilleran fold-thrust

Manuscript received March 19, 2002; provisional acceptance June 28 2002; revised manuscript received October 4, 2002; final acceptance January 20, 2003.

AUTHORS

L. Echavarria ~ *Conicet, Argentina, Cornell University; lechavar@mines.edu*

Leandro E. Echavarria received his Licenciado en Geologia degree (1992) and his Ph.D. (1997) from La Plata University (Argentina). He joined XR Consultants and worked as a field and structural geologist in the Subandes from 1998 to 2000. He spent two years as a visiting scientist at Cornell University working on the Subandes stratigraphy and structural geology. Now, he is a postdoctoral research associate at Colorado School of Mines.

R. Hernández ~ *XR Consultants, Argentina; hernandezr@sinectis.com.ar*

Roberto M. Hernández earned his Licenciado en Geologia degree from La Plata University (1980) and then specialized in petroleum geology at Buenos Aires University (1981). He worked for 12 years for YPF where he was chief of surface geology for the northwestern Argentina section. Since 1993, he has been an XR Consultants geologist in charge of the stratigraphic and structural studies in Bolivia and Argentina. At present, he is the manager of XR Exploracionistas Regionales y Servicios.

R. Allmendinger ~ *Cornell University; rwa1@cornell.edu*

Richard Allmendinger received his Ph.D. in structural geology from Stanford University in 1979. He joined the faculty at Cornell University in 1984, where he is now a full professor. He has worked in Andean geology since 1981 and also includes among his interests numerical modeling of fault related fold, analysis of fault populations, and neotectonics.

J. Reynolds ~ *Brevard College; reynoljh@brevard.edu*

Jim Reynolds holds A.B. and M.A. degrees and Ph.D. from Dartmouth College, United States. He has worked on the magnetostratigraphy of Argentine Neogene foreland basins since 1984 as a graduate student (1984–1987), a Fulbright Scholar (1989), researcher (1987–present), and consultant (1994–present). He is currently a geology professor at Brevard College in Brevard, North Carolina, United States.

ACKNOWLEDGEMENTS

We wish to thank the geologists of the Yacimientos Petroliferos Fiscales Commission 6 who started with the field data recompilation and analysis of the area, with special thanks to A. Di Salvo, A. Schulz, L. Constantini, and D. Starck. Tecpetrol and the UTE Aguaragüe provided the seismic information; we also thank Lic. Mario Alarcon for his help with the seismic lines. The manuscript was greatly benefited from valuable comments and suggestions by Teresa Jordan and *AAPG Bulletin* reviewers J. Verges, N. Hanks, and D. Wiltschko.

belt of the western United States. Shallow crustal shortening in the Subandean belt is generally thought to be directly associated with the majority of crustal thickening that produced the Altiplano, the great plateau of the central Andes (Isacks, 1988; Gubbels et al., 1993). Given this prominent role ascribed to the Subandean belt in most models of Andean orogenesis, it is particularly surprising that so little is known about the structural evolution of the belt.

Industry exploration has significantly improved our knowledge of the structural geometry of the Subandes during the past 20 yr (Mingramm et al., 1979; Baby et al., 1992; Belotti et al., 1995; Dunn et al., 1995; Starck and Schulz, 1996; Giraudo et al., 1999). The province is home to several major gas discoveries during the last 10 yr. Organic matter maturity and hydrocarbon generation are closely related with the burial depth, which is mainly controlled by the thickness of Neogene foreland basin deposits (Starck, 1995, 1999; Cruz et al., 2001). Because fault-related migration is thought to be contemporaneous with the deformation, a precise understanding of the timing of uplift of individual ranges in the Subandean zone relative to maturation history is crucial. The almost complete lack of detailed knowledge of the ages of motion of individual thrust plates hampers not only exploration in the region but also reduces models relating Subandean shortening to plateau uplift to mere speculation.

In this paper, we provide the first detailed chronology of motion for the southernmost Subandean belt in northern Argentina (22–23°S). Here, the main decollement located in Silurian shale dips 2–3°W and is accompanied by an important secondary detachment in the Devonian that has produced a unique geometry of lift-off folds on the crests of deeper fault-bend folds. Using regional balanced cross sections controlled by industry seismic reflection profiles, field geology, and magnetic reversal stratigraphy, we use different dating methods of thrust motion that include growth strata, vertical separation diagrams, accumulation rate history, facies migration, and unconformities to identify episodes of growth of each of the major structures. The resulting chronology combined with the kinematic models provides a detailed record of shortening rates and history of loading during the last 9 m.y.

STRUCTURAL GEOLOGY

The Subandean zone is a thin-skinned thrust belt characterized by elongated anticlines that trend north-northeast–south-southwest (Figure 2), forming several continuous, parallel ranges (Mingramm et al., 1979; Aramayo Flores, 1989, 1999; Belotti et al., 1995; Kley and Monaldi, 1999). The southern Subandean belt extends for about 600 km from the elbow of the Bolivian orocline at Santa Cruz de la Sierra, Bolivia, to northwestern Argentina. The main detachment level is in Silurian shale and has a 2–3°W dip. The properties of the Silurian shale, the configuration of long and thin ranges (Dunn et al., 1995), and the absence of shallow earthquakes suggest that it is a continuous and efficient decollement level. Important

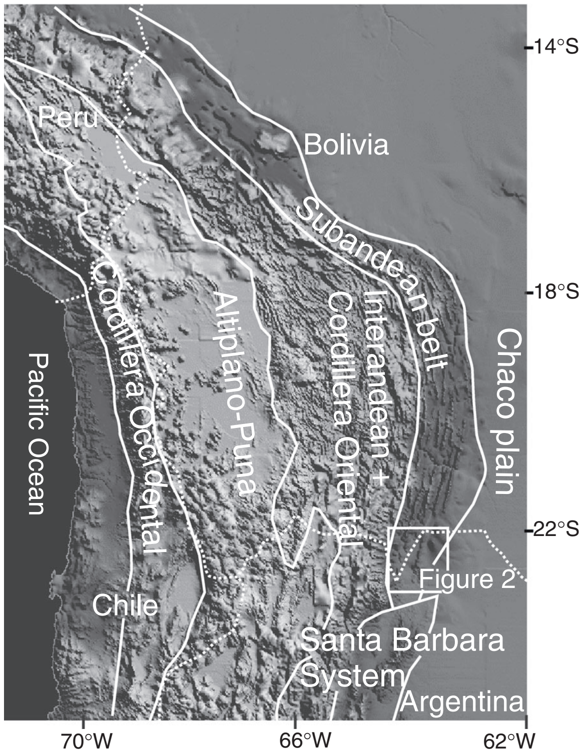

Figure 1. Regional setting of the studied area in the Central Andes, showing the topography and principal morphotectonic subdivisions. The rectangular area in the southeast corner is shown in Figure 2.

intermediate detachment levels occur mainly in the Devonian units (Baby et al., 1992; Belotti et al., 1995; Aramayo Flores, 1999; Leturmy et al., 2000). Their location is strongly controlled by the paleogeography and the distribution of fine-grained facies in the Devonian rocks. Because these facies are diachronous from east to west (Albariño et al., (2002), the intermediate detachment level cuts time lines and even sequence boundaries.

The presence of units with contrasting mechanical behavior allows us to divide the deformed column into three structural intervals (Figure 3) that approximately coincide with the lithotectonic units of Baby et al. (1992) and with the levels of Aramayo Flores (1999). In general, a lower competent level includes Silurian–Devonian shallow-marine strata deposited in a foreland-type basin east of the Ocloyic orogenic front (Isaacson and Diaz Martinez, 1995; Sempere, 1995; Starck, 1995); other authors suggest that it is a marine sag basin or back-bulge basin, with thermal subsidence (Vistalli, 1999; Albariño et al., (2002). It consists of several coarsening-upward packages, limited at the base and top by sharp contacts (Starck et al., 1992; Starck, 1995).

An intermediate incompetent structural level corresponds to a thick Upper Devonian shale that is well developed in the subsurface of the Argentine Subandean and Chaco plain where it is about 1000 m thick. The Devonian shale thins westward because of pre-Carboniferous erosion. This black laminated shale unit plays a fundamental role in oil generation. The lower part of this unit, approximately the first 200–250 m, may be attached to the lower structural level, whereas the upper 100 m may be included in the upper structural level (Aramayo Flores, 1999).

Finally, the upper structural level comprises the Tarija and Tertiary foreland basin deposits and acts in a passive way with respect to the deformation. The Late Carboniferous–Early Permian Tarija basin developed in deep paleovalleys eroded on the Devonian sequences, and its infill is made up by glacially derived continental deposits separated by unconformities (Starck et al., 1992; Starck, 1995). After the Gondwana glaciation, eolian sandstones interbedded with limestones accumulated during the Late Permian–Early Triassic (Sempere et al., 1992; Sempere, 1995), and eolian sandstones accumulated during the Jurassic. The Tertiary foreland basin deposits are described in detail in the following sections.

In a general way, all the major faults cut upsection from the basal detachment level, verging eastward and dipping westward (Figure 4). In the western Subandean ranges, where the intermediate structural level is reduced in thickness because of erosion, the deformation of the three structural levels is homogeneous. In the west, and everywhere in the lower structural level, the faults generate fault-bend anticlines with relatively broad crests, gentle backlimbs, and steeper forelimbs. Farther to the east, however, the Devonian shale that characterizes the intermediate structure level is more prevalent and thickens structurally by a factor of five or more in the cores of the anticlines, producing the decoupling between the lower and upper structural levels (Figure 5A). The apparently ductile behavior of this intermediate level is actually the result of numerous small faults and shear zones (Kley and Monaldi, 1999). The decoupling is incipient at the Pintascayo range and becomes more important to the east, at the Baja Orán, San Antonio, and Aguaragüe ranges (Figures 4, 5). Aramayo Flores (1989) has proposed that the minimum thickness of 500 m of the Devonian shale is required to produce the lift-off. In the eastern Subandean ranges, the upper structural level is characterized by folds with steeper flanks and narrow crests, with common box-fold geometries, and only bisected by minor faults. This

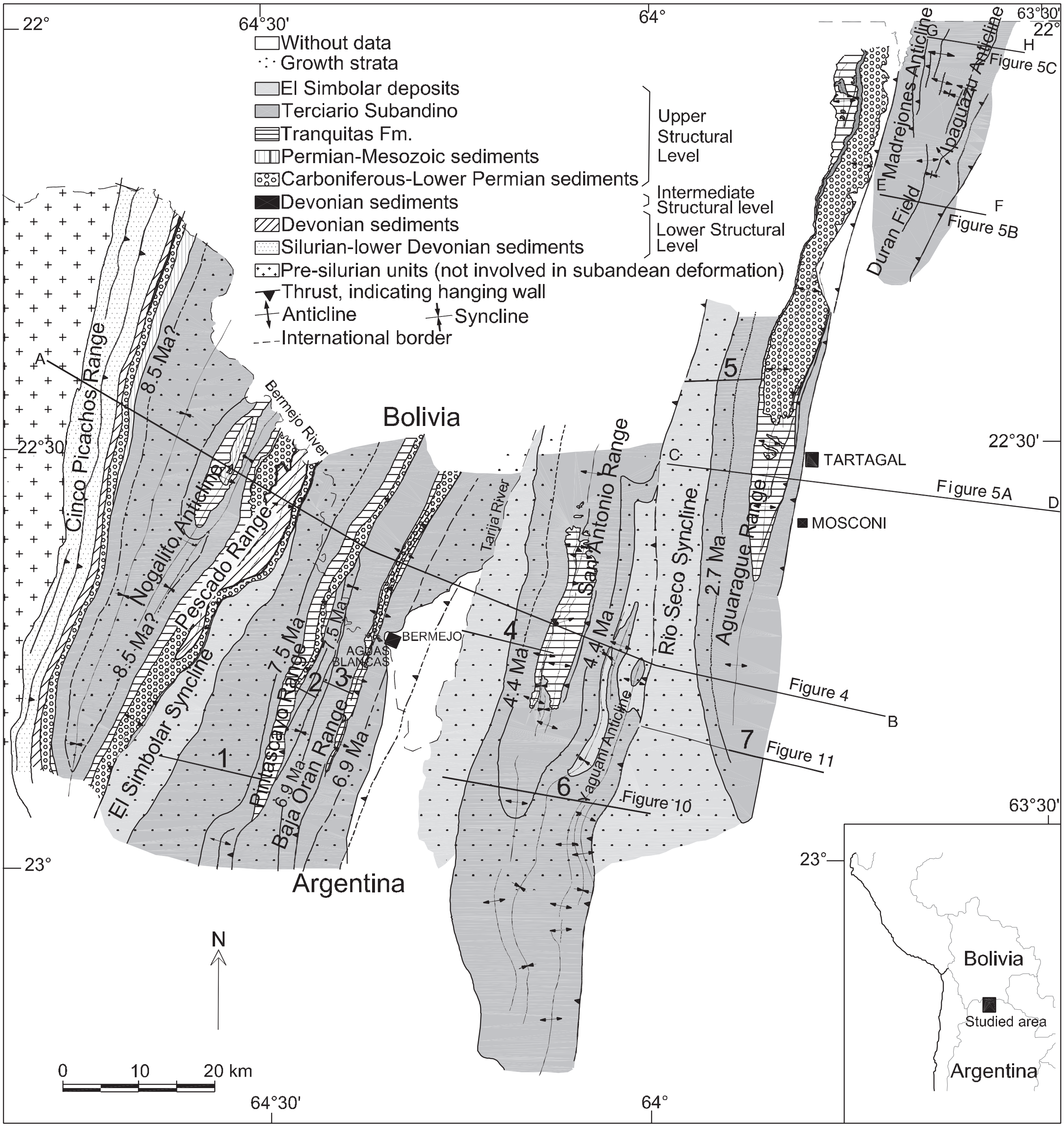

Figure 2. Location and simplified geologic map of the northwestern Argentina Subandean belt. Cross-section locations: AB, regional cross section (Figure 4); CD, Aguaragüe range cross section (Figure 5A); EF, Duran field cross section (Figure 5B); GH, Madrejones-Ipaguazu field cross section (Figure 5C). Magnetic-polarity stratigraphy section (Figure 7) locations: (1) Río Iruya; (2) Las Manzanas; (3) Peña Colorada; (4) La Porcelana; (5) Quebrada de León. Seismic lines location: (6) San Antonio range seismic line (Figure 10); (7) Aguaragüe range seismic line (Figure 11).

level passively adjusts its shape to the deformation imposed on it by the intermediate level.

The easternmost anticlines, e.g., Duran (Figure 5B), Madrejones, and Ipaguazu (Figure 5C), and the plunge regions of some other anticlines (e.g., Aguaragüe, Mombru and Aramayo Flores, 1986) have wide crests and gentle limbs. These broad anticlines appear to represent the initial stages in the anticlinal evolution. Increasing

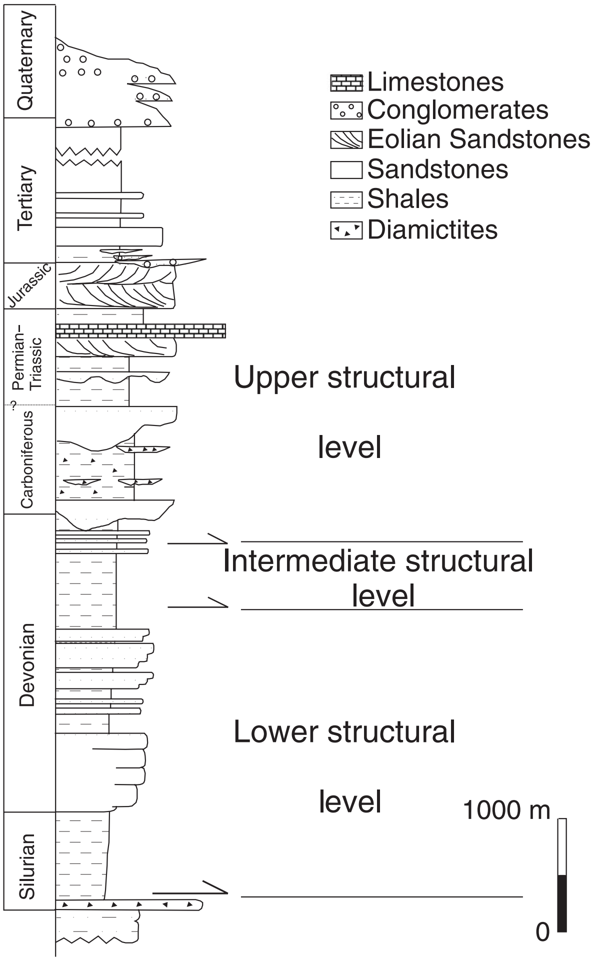

Figure 3. General stratigraphic column of the studied area, showing the main detachment levels that represent the boundary between the three major structural intervals.

shortening results in steeper flanks, well-developed stacking, and narrower crests (Figure 5A). In other words, different evolutionary stages are preserved from east to west (Kley and Monaldi, 1999), e.g., Duran-Aguaragüe-San Antonio, or from an anticline's plunge to its middle sector (e.g., Aguaragüe, from its south plunge to the north) (Figures 4, 5).

The disharmonic geometries produced by decoupling at the middle structural level are commonly interpreted as tectonic wedge geometries (Belotti et al., 1995). The major thrust rises from the basal detachment and joins a back thrust located at the base of the intermediate structural level, which acts as a passive roof thrust and as a detachment level for the intermediate and uppermost structural levels (Figure 5B).

The cross sections presented here (Figures 4, 5) were modeled with Trishear software (Allmendinger, 1998; Zehnder and Allmendinger, 2000) that facilitates the construction of parallel and similar folds over ramps as well as Trishear fault-propagation folding. Because the belt is characterized by broad synclines in which the stratigraphic thickness above the basal decollement is normal (Figure 4), each anticline can be modeled individually. Only in the case of the El Pescado range is some shortening transmitted forward to the Pintascayo range. Where decoupling across the middle structural level is important, the different fold kinematics at different levels required each to be modeled independently. All major faults propagate up from the basal decollement with low propagation to slip ratios (<2) while cutting across the Silurian shales. Where they reach more competent units, the tip line breaks rapidly across those units up to the base of the intermediate structural level; the already formed fault-propagation anticline is translated passively and ''inserted'' into the Devonian shales of the middle level, producing a wedge geometry.

Shortening varies along the strike of the Subandean thrust belt (Kley, 1998); south of the Santa Cruz elbow, the maximum published shortening is about 100 km (50–55%) near 21° latitude; if the Interandean zone is included (see Dunn et al., 1995; Giraudo et al., 1999), the value is about 156 km (56%). The regional cross section presented here (Figure 4) has a minimum shortening of about 60 km, including 5 km of shortening caused by the back thrust at the Cinco Picachos range (Starck and Schulz, 1996). From the minimum shortening of about 60 km, 65% is generated by faults in normal sequence of thrusting, and 35% is caused by out-of-sequence thrusting. This amount of shortening coincides with that found by other authors at approximately the same latitude: 60 km in the model of Mingramm et al. (1979), 55 km in Starck and Schulz (1996), and 50–55 km calculated by Schmitz and Kley (1997) and Kley and Monaldi (1999).

TERTIARY STRATIGRAPHY IN THE SUBANDEAN RANGES

The structural data presented above are interesting for their similarity to previously published estimates, but those studies lacked all but the crudest knowledge of the timing of the structures. To advance beyond this point and to further understand the thermal maturation history of the Subandean basins, the ages and growth relations of strata in the Cenozoic foreland basin of the Subandean belt must be determined. The Cenozoic foreland basin of northwestern Argentina comprises more than 7 km of mostly Neogene continental deposits (Figure 6) that have been described as

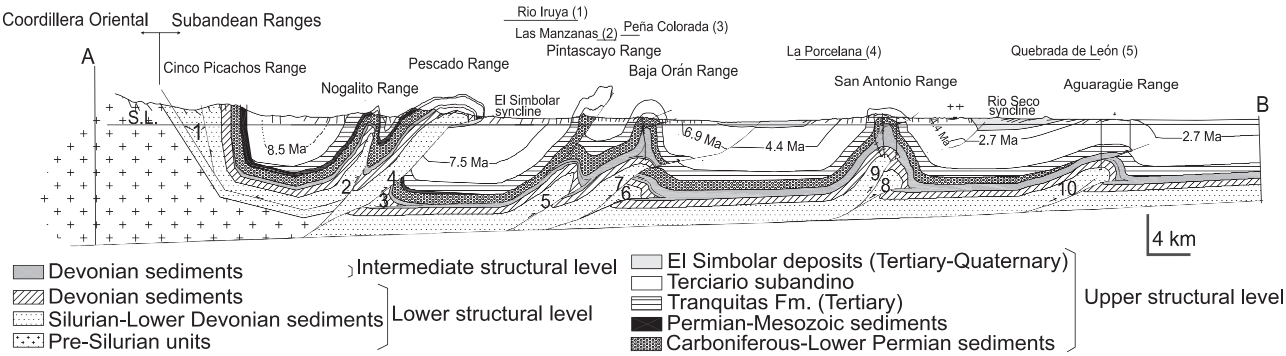

Figure 4. Balanced cross section across the entire Subandean thrust and fold belt. (1) Cinco Picachos back thrust; (2) Nogalito thrust: in-sequence with out-of-sequence reactivation; (3) Pescado thrust: in-sequence; (4) Pescado thrust: out-of-sequence; (5) Pintascayo thrust: in-sequence with out-of-sequence reactivation; (6) Baja Orán thrust: in-sequence; (7) Baja Orán thrust: out-of-sequence; (8) San Antonio thrust: in-sequence; (9) San Antonio thrust: out-of-sequence; (10) Aguaragüe thrust: in-sequence (with minor out-of-sequence reactivation?). The time lines shown in the Tertiary (based on volcanic ash geochronology and magnetic-polarity stratigraphy) represent the local boundary between the pregrowth and growth strata. Positions of magnetic-polarity stratigraphy sections are also shown. See Figure 2 for location. No vertical exaggeration.

Grupo Orán (A. Russo, 1975, personal communication). Prior to studies reported by Hernández et al. (1996, 1999), on which the following analysis is based, there were virtually no data that constrained the onset of foreland basin deposition in this environment. Furthermore, stratigraphic units are commonly diachronous, from north to south as well as east to west, getting younger to the south and east. A particularly vexing example is Miocene marine strata that were formerly interpreted as a single event fixing the beginning of Subandean deformation (e.g., Gubbels et al., 1993), but which now can be shown to be as old as 15 Ma and as young as 8 Ma in different parts of the belt (Reynolds et al., 2000; Hernández R., 2001, personal communication).

Overview of the Cenozoic Stratigraphic Sequence

The oldest Tertiary unit, the Tranquitas Formation, is about 850 m thick in the western Subandean ranges (Hernández et al., 1996) and about 750 m at the Aguaragüe range (J. J. Zunino, 1944, personal communication). Rocks beneath an erosional unconformity at the base of the Tranquitas are progressively older to the east and southeast. These nonmarine Tranquitas strata present distal facies at the base and become increasingly proximal upsection with lacustrine, ephemeral river and eolian facies (Hernández et al., 1996) (Figure 6).

Overlying the Tranquitas Formation, three depositional progradational cycles have been described (Hernández et al., 1996, 1999) in a thick column (>6000 m) of continental deposits, known as "Terciario Subandino" (J. J. Zunino, 1944, personal communication). In general, the facies of these terrestrial sediments correspond to four major depositional environments: alluvial fans, braided streams, distal ephemeral fan, and mud flat. The alluvial fan facies is characterized by polymictitic conglomerates, with clasts more than 15 cm in diameter, dispersed in a sandy quartz matrix. The beds are tabular, with erosive base, and internally cross-bedded or planar laminated. The braided stream facies consists of fining-upward sets of coarse-grained sandstones or conglomerates arranged in thin to medium beds, with erosive base, cross laminations, displaying channel bars and sand-wedge structures. The conglomerate beds are scarce at the base of the Terciario Subandino, but increase in volume upward, and they are the predominant lithology in the upper 15% of the unit. Beds with variable thickness between a few centimeters and several meters characterize the distal ephemeral fan facies. These sequences have channel facies at the base represented by moderately sorted, coarse-grained sandstones, with poor cross-bedding. They become fine-grained upward, where red, fine-grained sandstones are commonly parallel laminated and locally have poorly developed climbing ripples. These latter red sandstones represent channel lobe and flooding facies on the ephemeral fan. The mud-flat facies, interpreted as flooding events (Hernández et al., 1996), are formed by red fine-grained sediments, commonly arranged in thin tabular beds, massive or parallel laminated, with climbing ripples.

The first progradational cycle deposits have wedge geometry, thinning to the east. Their thickness is about

1300 m at Río Iruya and 470 m at La Porcelana, disappearing completely at the west flank of the Aguaragüe range (Figure 7). This cycle comprises mud-flat facies at the base, coarsening upward to multistoried channel facies to the top.

A variable short-term depositional hiatus has been interpreted between the first and second progradational cycles at Río Iruya, Las Manzanas, and Peña Colorada (Figure 7). The second progradational cycle begins with fine-grained mud-flat facies and coarsens and thickens upward to channel-fill facies characterized by coarse- to medium-grained sandstones. The upper section is characterized by coarser facies, with anastomosing conglomerates where numerous plant fossils are found. These facies, known informally as La Maroma, are braided fluvial systems related to a more humid climate with permanent rivers. Intercalated with the described sediments are several ash-fall tuff beds. They are fine-grained, commonly biotite-rich, gray tuffs, which have been isotopically dated at different locations in the basin, ranging in age from 8.56 to 5.92 Ma. Their mineralogical differences are the basis to distinguish guide beds (Viramonte et al., 1994). This depositional cycle ends with a conglomerate progradation of alluvial fan facies.

The third progradational cycle overlies the second progradational cycle, separated by a gentle erosional unconformity. The thickness and facies arrangement of this cycle vary considerably between different synclinal depocenters (intermontane valleys) as well as along the strike of the intermontane basins. In general, this cycle also displays a coarsening- and thickening-upward pattern, with fine- to medium-grained, poorly sorted deposits at the base that prograde upward to braided streams and alluvial fans. A remarkable flooding event characterized by shales and fine-grained sandstones is present in the middle of the third progradational cycle at Río Iruya (between the 5400- and 5800-m level at the Río Iruya section, Figure 7), which is not recognized in other locations to the east, nor in other localities at the same structural position, as is the El Nogal column (27 km north of Río Iruya, Figure 2).

Finally, a growth unconformity is present in all the intermontane basins. It is the most prominent unconformity observed in northwestern Argentina's Neogene foreland basin and is recognized in the field by a sudden appearance of monotonous coarse-grained alluvial fan conglomerates that are known as El Simbolar, and by changes across the unconformity surface in bed strike and dip.

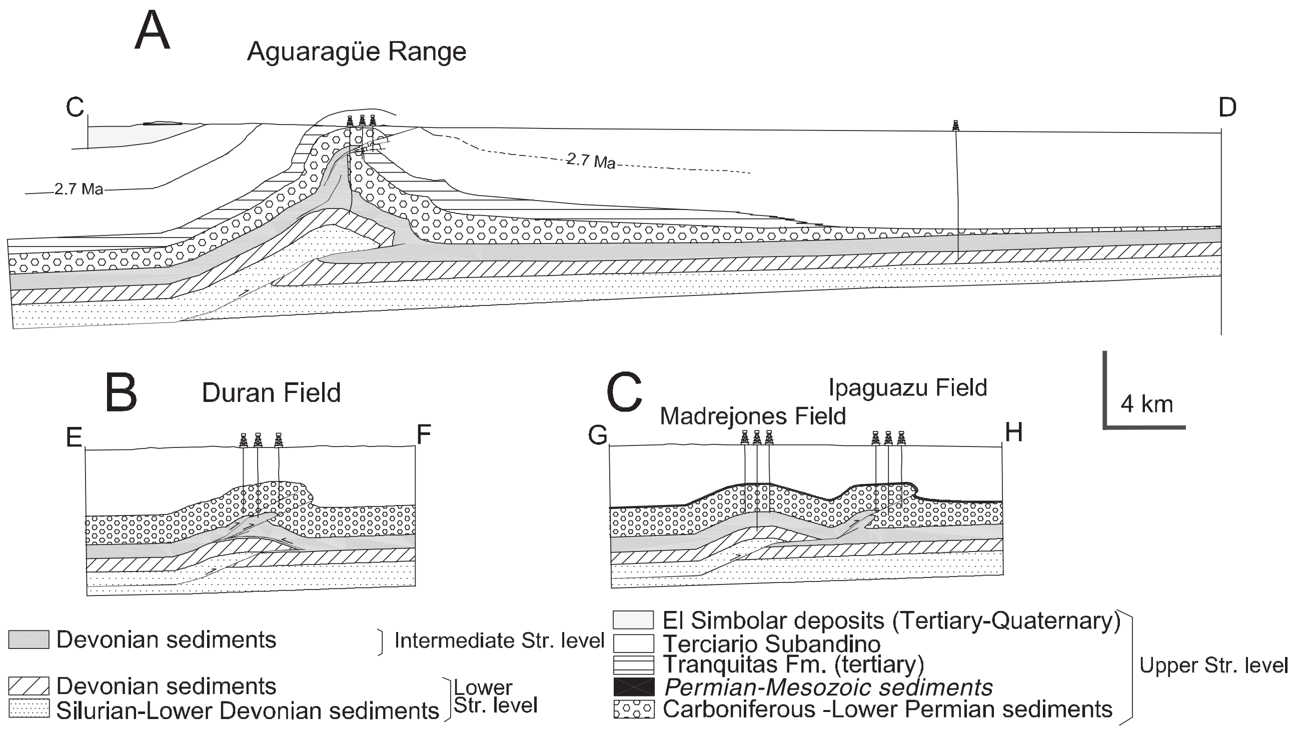

Figure 5. Aguaragüe range (A), Duran (B), and Madrejones-Ipaguazu (C) fields cross sections. Modified after Belotti et al. (1995). See Figure 2 for location. No vertical exaggeration.

Figure 6. Simplified stratigraphic column of the Cenozoic foreland basin deposits.

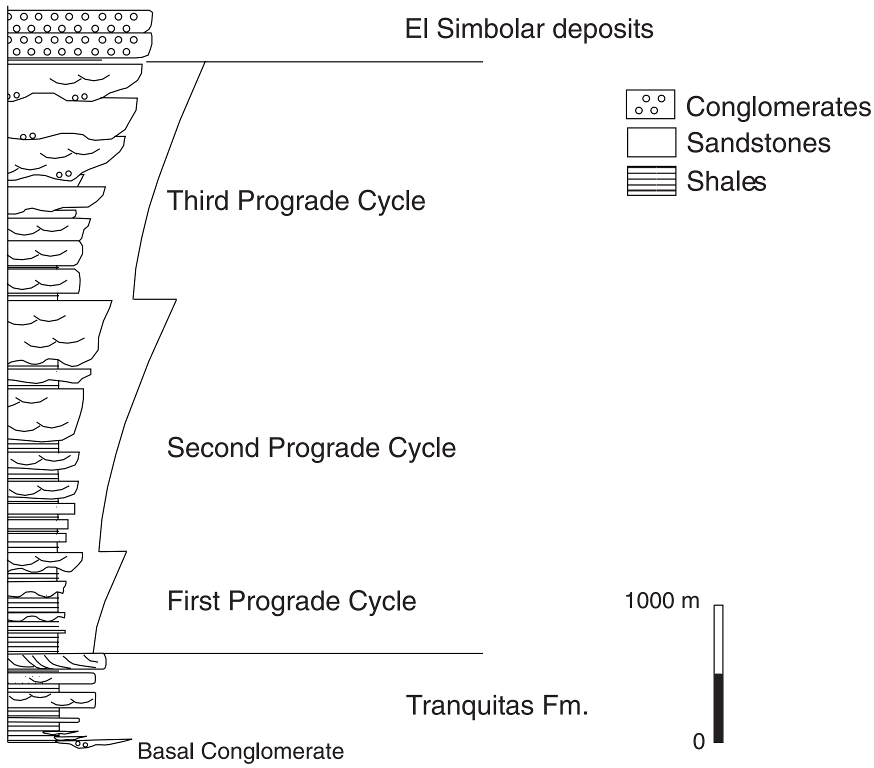

High-Resolution Chronology of the Tertiary Foreland Deposits

Five detailed stratigraphic columns with magnetic-polarity stratigraphy (Figure 7), some previously published (Hernández et al., 1996, 1999; Reynolds et al., 2001), provide a high-resolution chronology. To constrain the possible age of the strata, intercalated volcanic ashes were dated isotopically (Figure 7). The five sections are, from west to east (Figure 2), Río Iruya and Las Manzanas located at the back- and forelimbs of the Pintascayo range, respectively; Peña Colorada, situated at the backlimb of Baja Orán range; La Porcelana, in the west limb of the San Antonio range; and Quebrada de León, located on the backlimb of the Aguaragüe range.

The accuracy and precision of magnetic reversal stratigraphy are limited by the spacing between samples, rates of accumulation, accuracy of the global magnetic-polarity timescale (Cande and Kent, 1995), and duration of the polarity zone. In this study, the separation between samples ranges between 15 and 40 m on the initial pass, with resampling in the sites of most problematic correlation. Although the Tranquitas Formation was sampled, high-quality data results were not obtained, possibly because of a high degree of thermal alteration.

Applied Methods of Dating Thrust Belts

In this paper, we used several different methods for dating thrust motion. The most direct and straightforward ones are crosscutting relations and growth strata. However, other data derived from foreland basin deposits provide very useful constraints on thrust motion, although they are more ambiguous and imprecise. These methods are, in order of increasing ambiguity (Jordan et al., 1988), unconformities, provenance (Steidtmann and Schmitt, 1988), accumulation rate history (Johnson et al., 1985; Raynolds and Johnson, 1985; Johnson et al., 1986), and migration of facies (Flemings and Jordan, 1990; Jordan, 1995).

Crosscutting Relations

Crosscutting relations are not abundant, at least in this part of the Subandean zone, mainly because of high preservation rates and important structural decoupling at the Devonian shales level. Most of the major faults cutting up from the detachment level are blind. Most of the emergent faults are clearly interpreted as out-of-sequence faults, or at least with important out-of-sequence reactivations, they commonly cut even Pleistocene levels.

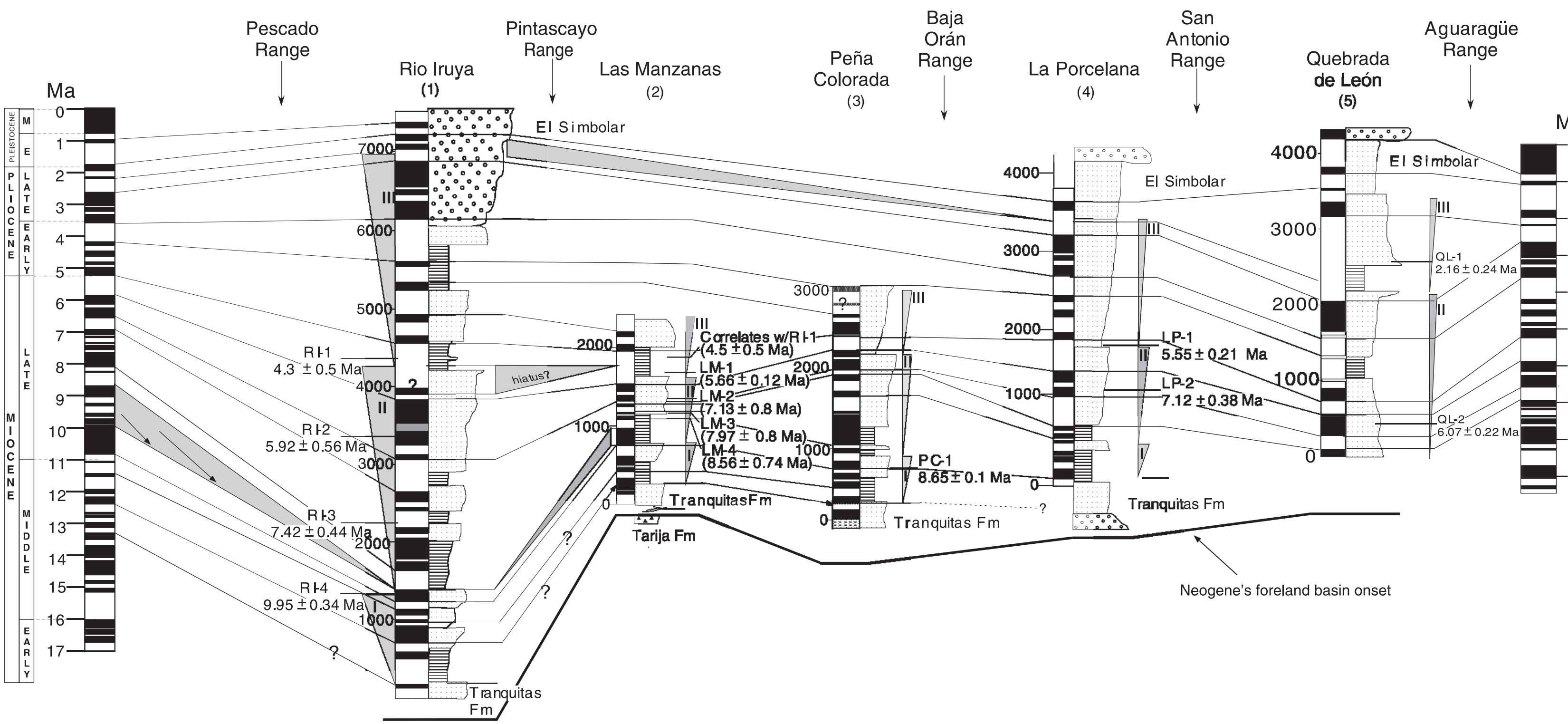

Figure 7. Correlation of the Río Iruya, Peña Colorada, Las Manzanas, La Porcelana, and Quebrada de León magnetic-polarity stratigraphy with the magnetic polarity timescale of Cande and Kent (1995). Positions in each column of isotopically dated volcanic ash are also shown. See Figure 2 for location of the five stratigraphic sections. Vertical scales posted on stratigraphic columns are in meters.

Growth strata

Growth strata (Medwedeff, 1989) that accumulated during and in the vicinity of growing structures facilitate remarkably precise dating of individual thrust movement histories in the Argentine Subandes. Growth strata are commonly recognized on the basis of their cross-sectioned geometries (Anadón et al., 1986; Medwedeff and Suppe, 1986; Suppe et al., 1992; Hardy et al., 1996), but in the Subandean ranges, geometries at the scale of fold limbs are difficult to document. At the surface, geometries are obscured by vegetation, and in the subsurface, the seismic data are of sufficient quality only at San Antonio and Aguaragüe ranges. Farther west at Pintascayo and Baja Orán ranges, the seismic resolution decreases dramatically mainly because of the steep anticlinal limbs. Nevertheless, because the age of the strata is quite precisely known with magnetic-polarity stratigraphy calibrated with ash chronology, the onset of the synorogenic strata is defined by vertical separation diagrams from surface data. The vertical separation diagrams are a columnar representation of pregrowth and growth strata.

Unconformities

The unconformities in the Subandean Tertiary are commonly hard to recognize. They are represented at the base of the prograding depositional cycles by erosional surfaces and sudden facies migration. On the basis of the available chronology, these erosional surfaces represent brief periods of time. The most important unconformities are those directly related to the growth of the structures.

Provenance

Sediment provenance is not a great help for differentiating individual thrust motions in the Subandes, mainly because of the small lithologic contrast along the entire thrust and fold belt. However, considering the contrast in bedrock lithology between the Cordillera Oriental and Subandean ranges, some interpretations can be made by the first appearance of diagnostic lithologies and by changes in abundance of modal classes. Hernández et al. (1996) described the sediments provenance area for the different sequences at the western Subandean ranges (Río Iruya position).

Accumulation Rates

If the accumulation rates of strata can be related to the rate at which the basement subsided, then with high-resolution chronology of foreland basin deposits, we can identify times of accelerating or decelerating tectonic subsidence. However, sediment accumulation is not only because of tectonic driving forces, it also reflects changes in the elevation of the depositional surface. Particularly in nonmarine strata, evidence for the elevation of the depositional surface is seldom preserved, so it is difficult to correct the accumulation data for elevation.

Facies Migration

There are many examples of the use of lateral facies changes and their migrations through time to date thrust movements (Wiltschko and Dorr, 1983; Bilodeau and Blair, 1986; Heller et al., 1986; Jordan et al., 1993). Jordan et al. (1988) concluded that interpretations of the histories of specific thrusts based only on facies distribution and migration should be avoided. The results of this study clearly underline the conclusion that the facies migration generally does not coincide with the thrust chronology obtained from other sources.

One can conclude that none of the described methods alone can solve the problem of determining the time of motion of individual thrusts in a thrust belt. In this paper, we combine several methods to establish the chronological evolution of the Subandean thrust belt much more precisely than before.

TIMING OF UPLIFT IN THE SUBANDEAN RANGES

Deformation in the Cordillera Oriental ended at about 10 Ma (Jordan and Alonso, 1987; Gubbels et al., 1993; Schmitz and Kley, 1997) and subsequently propagated into the Subandean ranges. There is some agreement that, until 6 Ma, there was little deformation in the Subandean belt (Moretti et al., 1996), but little is known about the ages of movement on individual faults. Here we provide the most accurate data yet bearing on the evolution of the Subandean thrust belt of northwestern Argentina.

The sections at Río Iruya (Figure 8A), Las Manzanas (Figure 8B), and Peña Colorada (Figure 8C) display dramatic increases in sedimentation rate starting between 8.5 and 9 Ma. Although the exact cause cannot be determined, we suggest that the rate increase was an indirect consequence of the formation and subsequent displacement along a major thrust ramp cutting out of basement and along a detachment horizon located at the Silurian shales. The hanging-wall ramp is located approximately beneath the Cinco Picachos range (Figures 4, 12A), and the matching footwall ramp

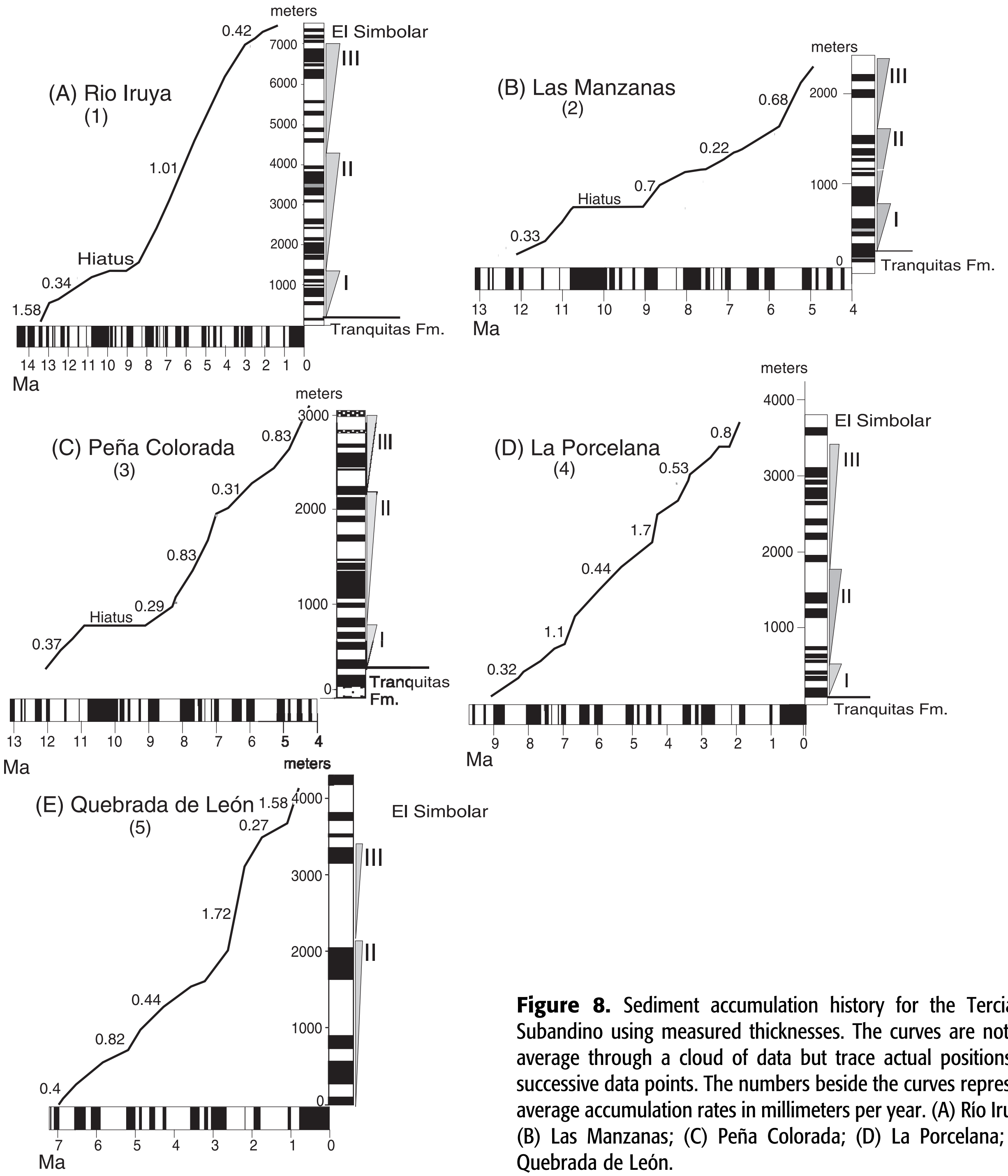

Figure 8. Sediment accumulation history for the Terciario Subandino using measured thicknesses. The curves are not an average through a cloud of data but trace actual positions of successive data points. The numbers beside the curves represent average accumulation rates in millimeters per year. (A) Río Iruya; (B) Las Manzanas; (C) Peña Colorada; (D) La Porcelana; (E) Quebrada de León.

may be located between 65 and 75 km farther west (Starck and Schulz, 1996; Allmendinger and Zapata, 2000). Movement over the footwall ramp brought crystalline basement from midcrustal levels over the Silurian detachment horizon (Allmendinger and Zapata, 2000), producing crustal flexure. That tectonically induced subsidence caused the increase in the sedimentation rate in the foreland basin extending eastward to the position of the Aguaragüe range. Some authors relate the acceleration of sedimentation rates at about 10 Ma (Marshall et al., 1993; Kley et al., 1997), here constrained to 8.5–9 Ma, to an explosive felsic magmatism event in the Altiplano and Western Cordillera Oriental at the same time (Sempere et al., 1990; Coira and Caffe, 1999). Rapid subsidence also produced facies migration and the deposition of fine-grained mud-flat sediments at the base of the second progradational cycle at Río Iruya, Las Manzanas, and Peña Colorada (Figure 7). It might also be related to the transgression of the Paranense Sea (Marshall et al., 1993; Ramos and Alonso, 1995; Rasanen et al., 1995), which is not well documented in this part of the Argentine Subandean belt (it might be represented by fine-grained strata in the Tranquitas Formation at the Aguaragüe region), but is well exposed in southern Bolivia, where Marshall et al. (1993) suggest that it developed some time between 10 and 8 Ma.

We propose that the above described early phase of shortening was transmitted along the footwall flat in the future Silurian level decollement to the Subandean area, generating a back thrust at the Cinco Picachos range (Figure 2). This back thrust occurs just at the forelimb of the megafault-bend fold cored by crystalline basement (Figure 4). This event probably also produced the proto-Pescado range uplift, although the rate of uplift must have been less than the rate of sedimentation (Figure 12A), at least locally, as is demonstrated by the clast provenance from Cordillera Oriental at the El Simbolar syncline (Hernández et al., 1996).

Farther east, growth strata geometries on seismic reflection data are extremely subtle, requiring a different approach. Therefore, at the Pintascayo and Baja Orán ranges, we constructed vertical separation diagrams (Bischke, 1994; Echavarria and Allmendinger, 2002). These diagrams (Figure 9), based on surface data, relate accumulated sediment thicknesses in two different locations at a specific age. They represent the vertical distance between layers of the same age at two different localities leveled at present time. When deposition rates are equal in the two localities, the vertical separation remains constant, but when they differ, an inflection in the vertical separation curve occurs, indicating the onset of the growth strata domain. The vertical separation curves are based on the magnetic stratigraphy columns (Figure 7).

In the Río Iruya–Las Manzanas diagram (Figure 9A), sedimentation rate was equal in both columns (constant vertical separation) until 7.6 Ma, but from this time onward, there is an important inflection in the vertical separation curve, indicating that the Pintascayo range began to grow (with respect to Las Manzanas section) at about 7.6 Ma. The inflection in the vertical separation diagrams for Peña Colorada–La Porcelana (Figure 9D) and Río Iruya–Peña Colorada (Figure 9C) at about 6.9 Ma may reflect the beginning of growth at the Baja Orán range. The vertical separation diagram for Las Manzanas and Peña Colorada columns (Figure 9B) also shows the inflection of the curve that corresponds to the Pintascayo range uplift, at about 7.6 Ma, and to the Baja Orán range uplift, at about 6.9 Ma.

Uplift of both Pintascayo and Baja Orán ranges forced the foreland basin to migrate to the east and produced a new subsidence event at the location of the La Porcelana section (Figure 8D) recorded as an abrupt increase in the sedimentation rate at about 6.9 Ma. Both the Pintascayo and Baja Orán ranges apparently continued growing simultaneously, resulting in less accommodation space in the syncline located between them. However, rapid subsidence and accommodation rates in the individual basins also developed to the west at the El Simbolar syncline (Figure 8A) and to the east in the simple foreland basin (La Porcelana location, Figure 8D). There, the accumulation rates are approximately 1 mm/yr between 7 and 6 Ma. However, in the intermontane basin between Pintascayo and Baja Orán ranges Figure 8B, C) the accumulation rates are only about 0.3 mm/yr, thus explaining the great difference in thickness between the anticline's limbs. At about 5–4.5 Ma (Figure 12A), the Pintascayo range might have had a considerable height, causing one or several rivers coming from the west to be dammed and the flooding of the El Simbolar intermontane basin. This event is observed in the Río Iruya section (Figure 7).

Deformation continued migrating eastward with the beginning of the San Antonio range uplift. Growth strata interpreted in seismic lines on the forelimb of the San Antonio anticline display onlap patterns to the west and divergence to the east (Figure 10). It is remarkable that these reflectors are not affected by the Yaguani anticline's (Figure 2) growth, which may be folded in a later deformation episode. The growth strata indicate that the beginning of the San Antonio range uplift was between 4.5 and 4 Ma, an interpretation similar (although not exactly the same) to that proposed by Mosquera (1999). Based on the growth strata observed on seismic lines, he proposed the onset of the San Antonio range uplift between 3.5 and 4 Ma. Our ages of 4.5–4 Ma correlate well with an important increase in the sedimentation rate (from 0.44 to 1.7 mm/yr) at about 4.4 Ma in the La Porcelana (San Antonio range backlimb) section (Figure 8D). This change also produces the inflection in the vertical separation curve in the La Porcelana–Quebrada de León diagram (Figure 9E), at about 4.5 Ma, and can also be responsible for the abrupt decrease in the vertical separation at 4.4 Ma in the Peña Colorada–La Porcelana diagram (Figure 9D). The end of growth in the San Antonio range cannot be

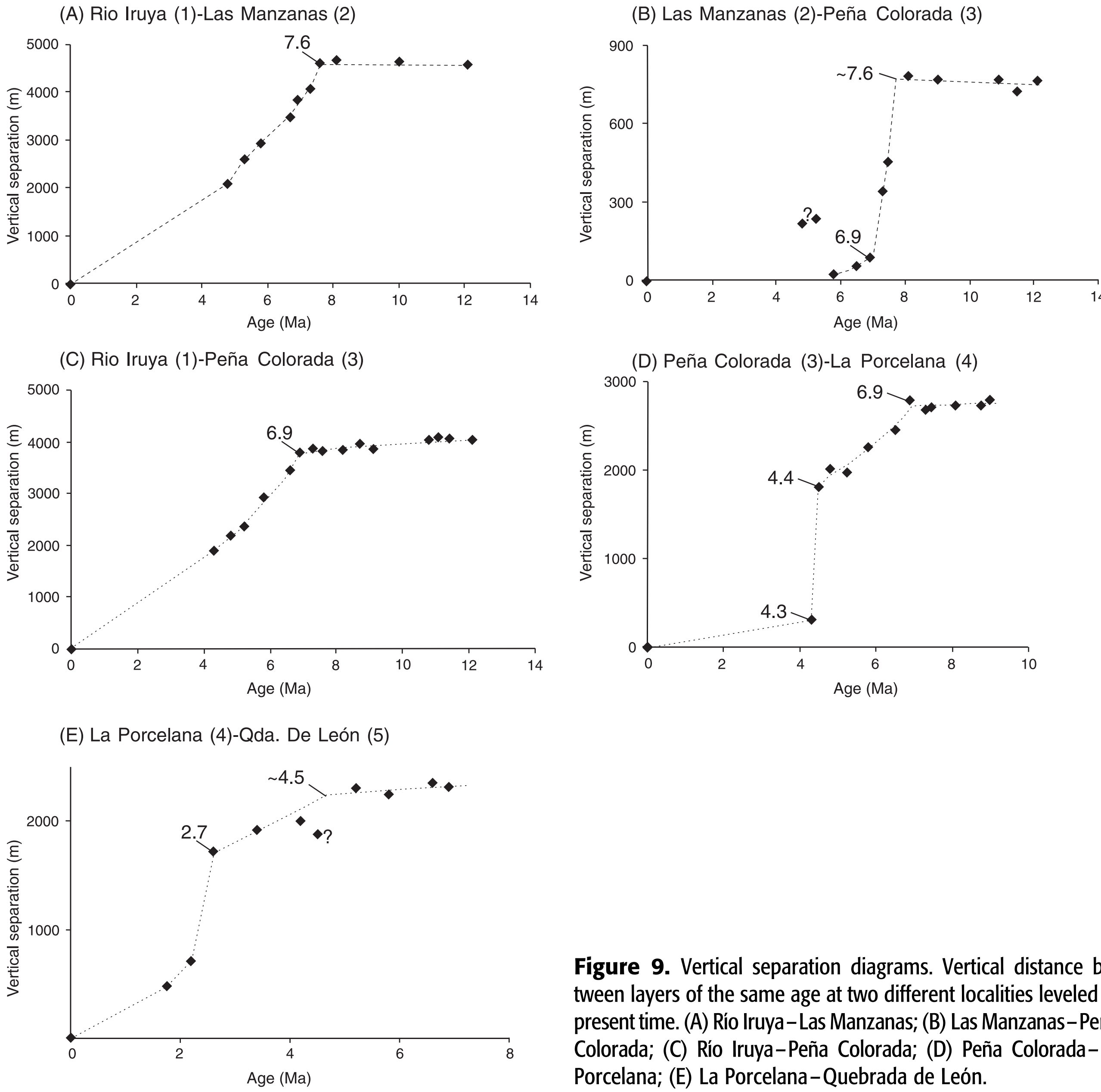

Figure 9. Vertical separation diagrams. Vertical distance between layers of the same age at two different localities leveled at present time. (A) Río Iruya–Las Manzanas; (B) Las Manzanas–Peña Colorada; (C) Río Iruya–Peña Colorada; (D) Peña Colorada–La Porcelana; (E) La Porcelana–Quebrada de León.

determined accurately, but it postdates 3.2 Ma, based on a smooth deflection in the La Porcelana section sedimentation rate curve at that time (Figure 8D).

Farther to the east at the Aguaragüe range, only poorly developed growth strata patterns are recognized in seismic sections, including some unclear reflectors that onlap the backlimb of the Aguaragüe anticline, and some reflectors that diverge to the west, which have been interpreted as progressive limb rotations. The ages assigned to these reflectors are about 1.5 Ma (Figure 11). Mosquera (1999) also describes growth relations on both limbs of the Aguaragüe anticline with ages between 2.5 and 3 Ma. The sedimentation rate diagram constructed for the Quebrada de León in the Río Seco syncline shows an abrupt increase in the sedimentation rate from 0.4 to 1.7 mm/yr at around 2.7 Ma (Figure 8E), followed by a facies migration to fine-grained facies of the base of the third progradational cycle. The onset of Aguaragüe range uplift can be restricted to 2.5–3 Ma, with ''in-sequence'' growth at least until 1.2 Ma.

All of the major anticlines had uplifted in sequence between 8.5–9 and 2.5 Ma (Figure 12A, B). However, continued thrusting resulted in increased complexity as recorded by the El Simbolar deposits.

The unconformity beneath the El Simbolar deposits, the best exposed unconformity recognized in the

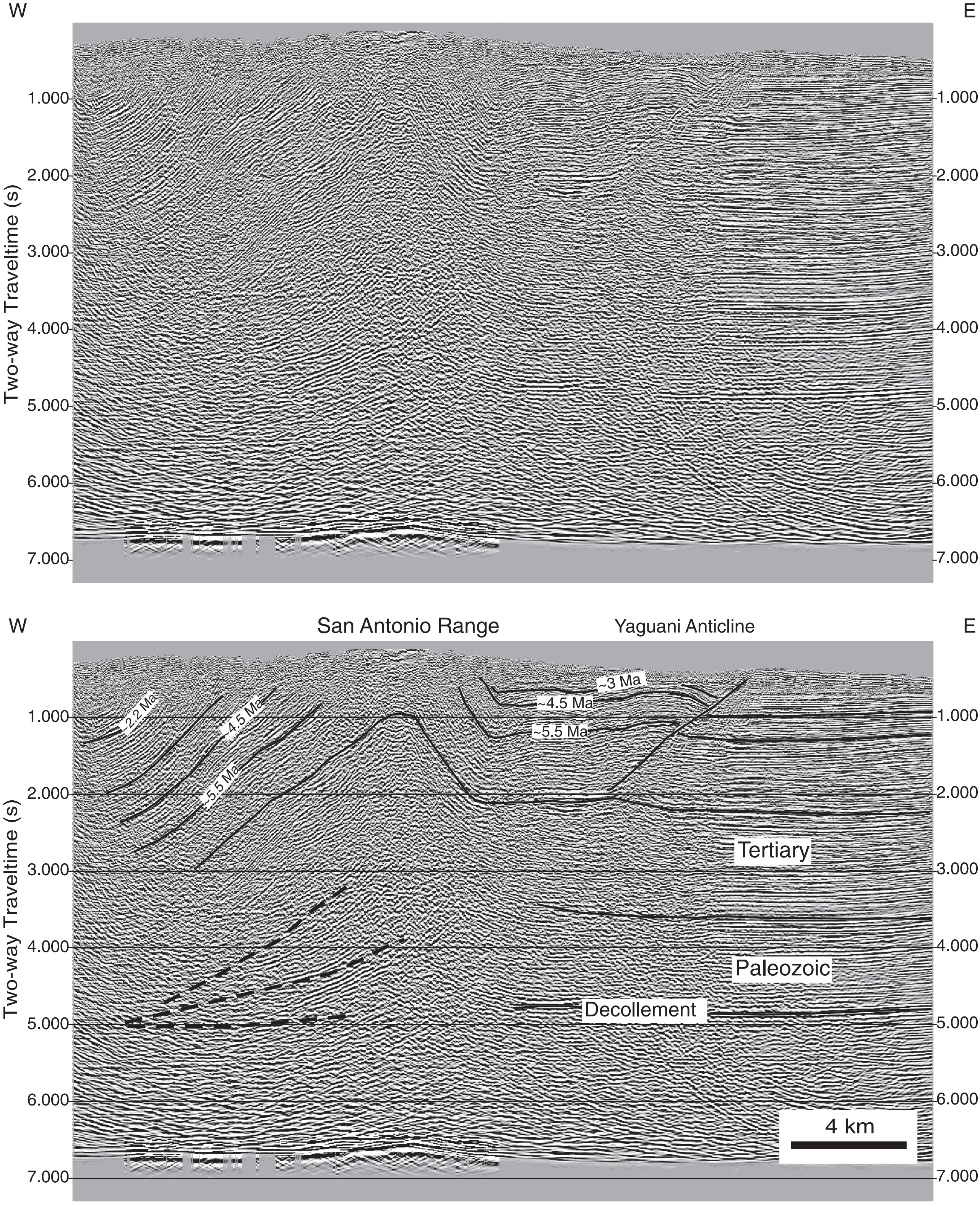

Figure 10. Uninterpreted and interpreted migrated seismic line showing growth relations at the front limb of the San Antonio range in strata whose ages are 4–4.5 Ma. Located in Figure 2 as line 6.

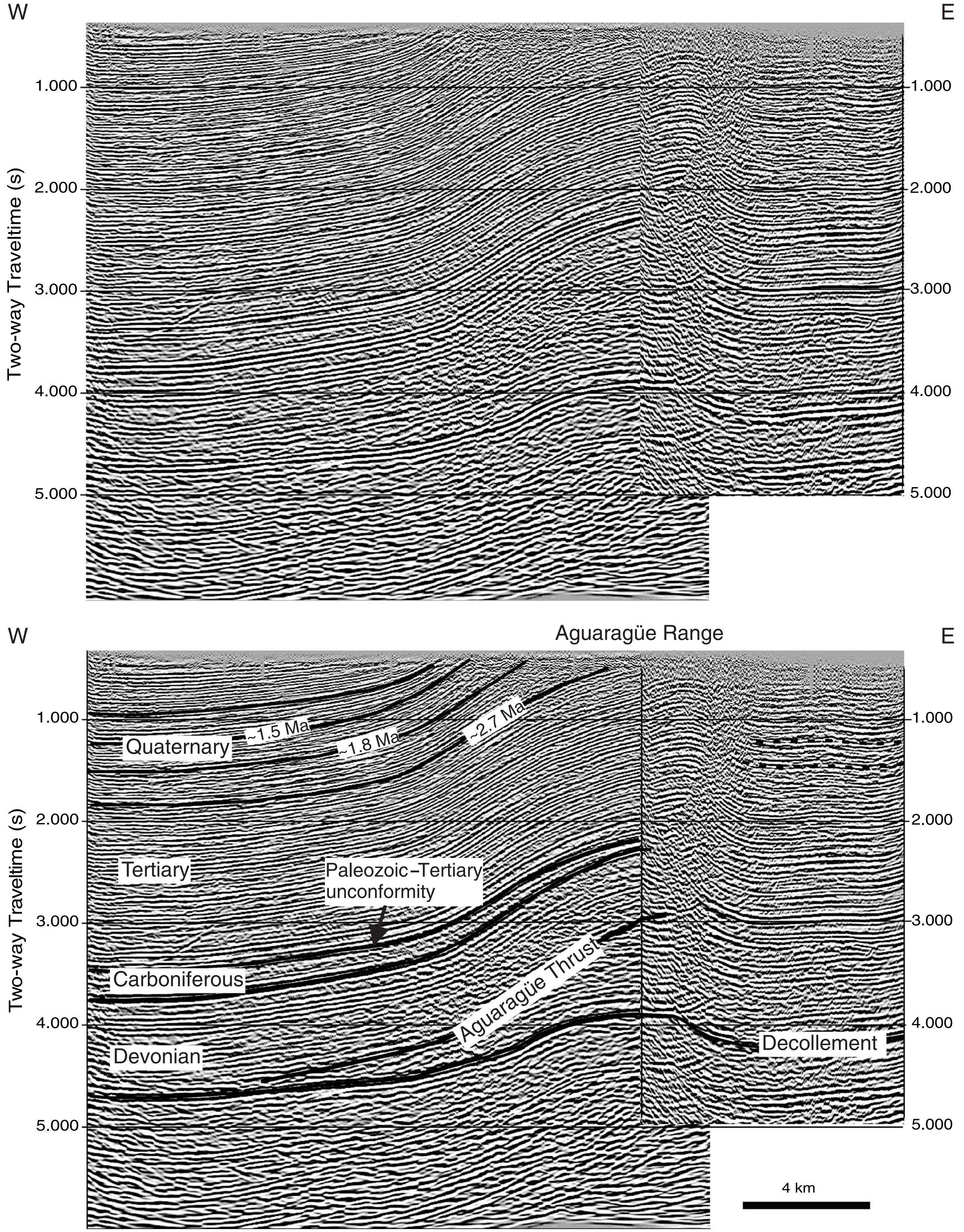

Figure 11. Uninterpreted and interpreted migrated seismic line of the Aguaragüe range. Progressive limb rotations at the back limb have been interpreted with ages of about 1–1.5 Ma. Located in Figure 2 as line 7.

northwest Argentine Neogene foreland basin, is characterized by a sudden facies migration, with alluvial fan progradation. The contrast of strike and dip of layers below and above the unconformity surface is quite notable. However, the unconformity is not always clear in seismic reflection lines except, for example, at El Simbolar syncline, where reflectors onlapping to the east have been described. In addition, as already mentioned, there are progressive limb rotations at the unconformity at the Aguaragüe range. Mosquera (1999) recognized the unconformity in the San Antonio and Aguaragüe anticlines, assigning an age of 1.8 Ma. The unconformity is recorded at La Porcelana section by a short hiatus (Figure 7) and posterior alluvial fan deposition at about 2 Ma. Finally, at Quebrada de León, the El Simbolar deposits accumulation correlates with the strong increase in the sedimentation rate at 1.2 Ma (Figure 8E).

The evidence that several ranges in the Subandean zone were uplifting with rates greater than the sedimentation rates during El Simbolar time leads to the interpretation that El Simbolar accumulated in isolated, range-bounded intermontane basins (Figure 12B). Correlation of the magnetic-polarity stratigraphy with the global magnetic-polarity timescale allows us to date the onset of the El Simbolar deposition at about 2–2.2 Ma at Río Iruya, 2–1.8 Ma at La Porcelana, and 1.2 Ma at Quebrada de León. The appearance of kilometer-scale series of alluvial fan facies conglomerates in a stratigraphic section is thought to indicate contemporary movement of nearby thrust sheets (Jordan et al., 1993). It seems likely that these alluvial fan facies were deposited in accommodation space generated by a new deformation event, which reactivated preexisting faults and formed new out-of-sequence ones. This event could have begun earlier than the deposition of the El Simbolar with the reactivation of the El Pescado fault at about 4.5 Ma, as is suggested by a change in sediment provenance from the Cordillera Oriental to the El Pescado range in the third progradational cycle at the Río Iruya location (Hernández et al., 1996). The appearance of El Simbolar facies at this position at 2–2.2 Ma may reflect acceleration in the erosional rates, probably because of climate changes. The out-of-sequence

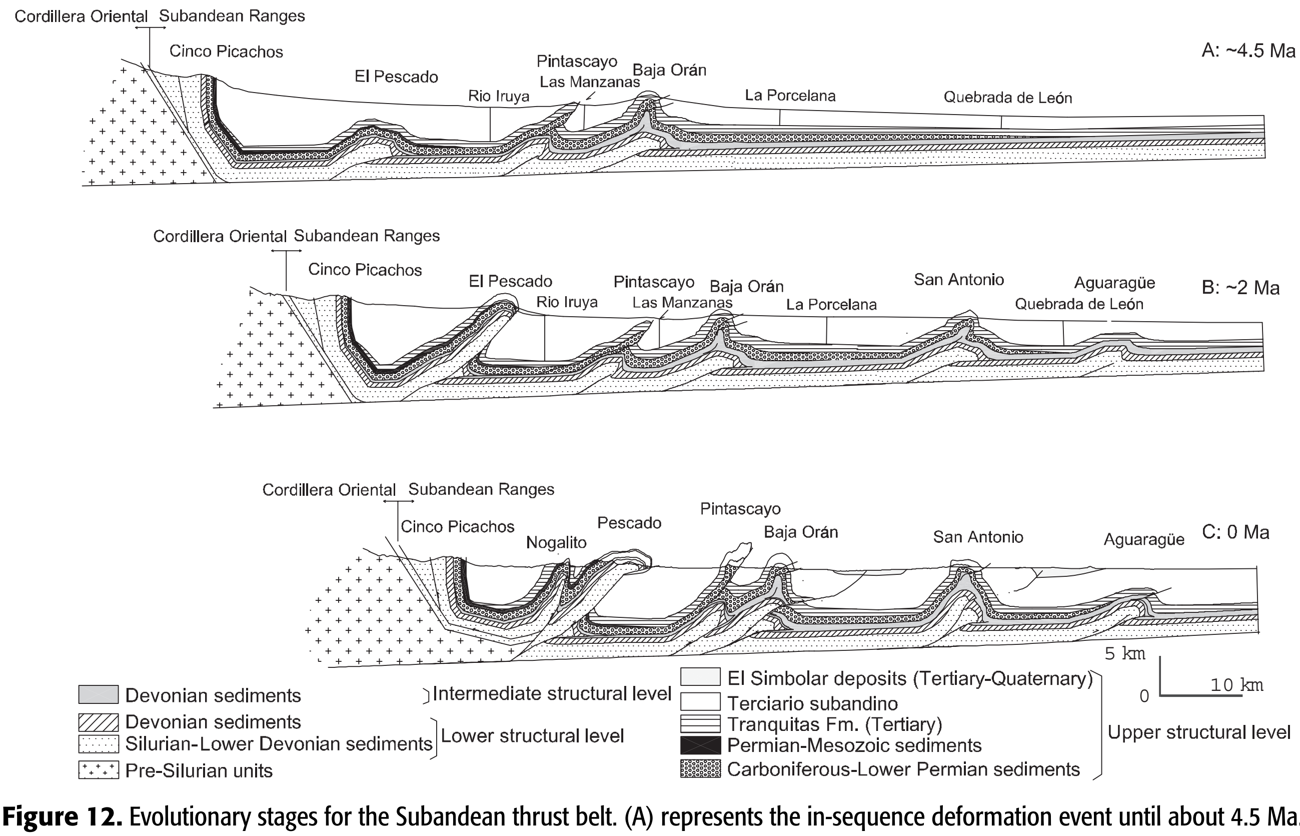

Figure 12. Evolutionary stages for the Subandean thrust belt. (A) represents the in-sequence deformation event until about 4.5 Ma., with the development of the Cinco Picachos range that represents the basement-cored mega-hanging-wall ramp, the proto-Pescado, Pintascayo, and Baja Orán ranges. (B) Uplift in-sequence of the San Antonio and Aguaragüe ranges, some out-of-sequence movements started at the west with the Pescado range uplift. (C) represents the present configuration.

movements migrated eastward, reaching the Aguaragüe range at approximately 1.2 Ma. These faults, which are out of sequence with respect to the deformation front, are simultaneous with respect to each other. Proof of activity continuing until the present can be found in the fact that the El Pescado fault cuts El Simbolar deposits dated at less than 1 Ma, and in the Quaternary strata tilted 8° with respect to the present fluvial terraces (Hernández et al., 1996).

UNCERTAINTIES IN THE CHRONOLOGY OF THE DEFORMATION

The sequence of deformation presented here, as in most similar studies, is based mainly on the age of the foreland basin sedimentary deposits related to the thrust and fold belt. There are no direct age determinations for the deformation itself, a fact that can produce uncertainties in the results. One of the errors is related to the accuracy of the magnetic-polarity stratigraphy and related isotopic dates of intercalated ashes. In this case, the magnitude of the error generally depends on the spacing between samples, rates of accumulation, and accuracy of and correlation with the global polarity timescale. Magnetic-polarity stratigraphy is, nevertheless, one of the most accurate methods for dating terrestrial sequences, where the estimated uncertainty on the age assigned to any magnetic-polarity zone is commonly less than 100,000 yr. Such errors are very small for the purposes of this study.

The greatest uncertainties are those derived from the degree of correctness of the geologic interpretations. For example, it is unclear whether certain major facies changes reflect deformation stages or are a response to other causes, e.g., river evolution or migration, which are semi-independent of the deformation. In addition, increased accumulation rates can be due to thrust loading or other causes like climate change or river migration, and even if deformation is the cause, we still do not know exactly which thrust produced the tectonic load that finally generates the subsidence.

For some thrusts like the Cinco Picachos range back thrust, there is little information about the timing of motion. In this case, the movement could be related to the first stage of Subandean deformation, or the fault might have been active for most of the Subandean deformational history.

The onset of the El Pescado thrust reactivation is another key point for which the uncertainty is quite high. If we consider this thrust to be completely related to the El Simbolar deposits, its motion might have started at 2.2 Ma. However, provenance studies (Hernández et al., 1996) indicate that in the third cycle at the Río Iruya, sediment provenance changes from the Cinco Picachos to El Pescado range. If these data indicate the emergence of the El Pescado range because of the onset of thrust reactivation, then the uplift of the range might be at about 4.5 Ma.

Another uncertainty is the lack of preservation of the sedimentary deposits. This is the case for the Las Manzanas and Peña Colorada sections (Figure 7), where the youngest preserved strata are 4.7 and 4.2 Ma, respectively. These columns cannot assist the identification of younger deformational events.

The general result is that the initial times of motion are better constrained than both the ages of the end of motion and the clues to establish continuous motion. In view of these unknowns, Figure 13A shows both the minimum and maximum time span over which each thrust was in motion. On the basis of these data, the deformation rate for the whole Subandean thrust and fold belt was calculated.

LATE CENOZOIC DEFORMATION RATES IN THE SOUTHERN SUBANDEAN BELT

By combining shortening estimates from our balanced cross sections for the southern Subandean belt with the age constraints just described, we can, for the first time, provide shortening rates with meaningful uncertainties (Figure 13B). Two rather different end-member interpretations result from this exercise. If we assume the maximum permissible duration of motion for each fault, then the shortening rate increased gradually and approximately linearly from its inception about 9 Ma until it reached its maximum rate of 11 mm/yr at about 3 Ma, with a modern rate of 8 mm/yr. If we assume the minimum duration of thrusting permitted by the data, then the curve indicates that the Subandean belt formed in two relatively discrete pulses of deformation around 9–7 Ma and from 2 Ma to the present. In this latter interpretation, shortening rates during the pulses may have reached 13 mm/yr or more, whereas in between pulses (7–2 Ma), shortening proceeded at a background rate of 0–5 mm/yr.

Coudert et al. (1995) carried out tectonic subsidence and crustal flexure studies in the eastern margin of the Subandean in southern Bolivia. Using poor age constraints, they suggest three stages of subsidence: relatively high rates between 10–9 and 7.5 Ma, and

Figure 13. (A) Duration of movement of individual thrusts of the Subandean belt. Both possible maximum and minimum duration that are consistent with the data set are shown. (B) Cumulative rate of motion for the complete thrust and fold belt as a function of time. The curves are drawn from the two interpretations presented in (A).

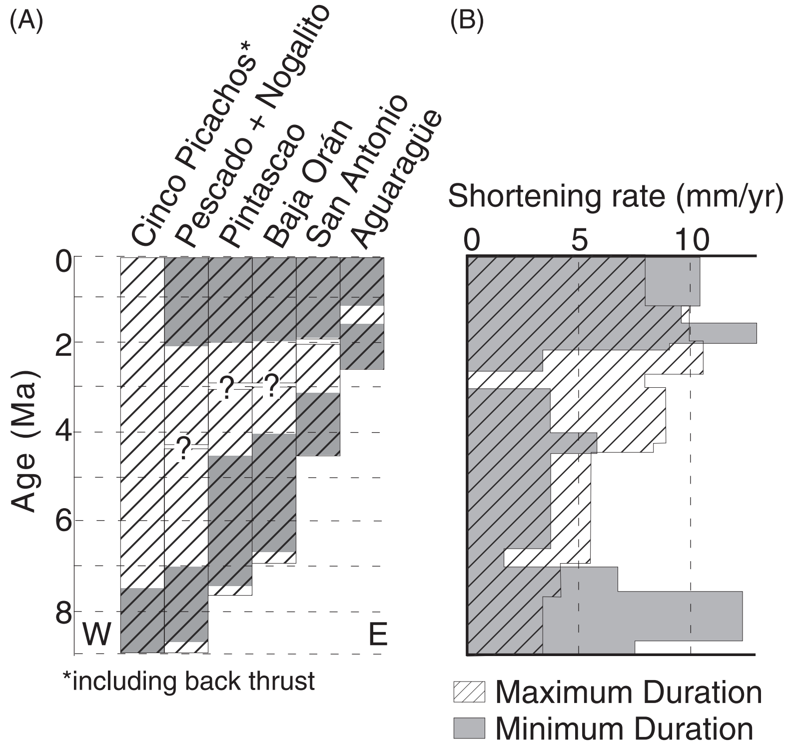

between 1 Ma and present, and an intermediate period of lower subsidence rate between 7.5 and 1 Ma. These rates correlate reasonably well with the thrust shortening rate history that we derive from our minimum duration model. Unfortunately, we cannot make a detailed comparison between our rate histories and the Nazca–South America plate convergence history because of the poor resolution of magnetic stripes on the Nazca sea floor.

In both scenarios presented here, horizontal shortening rates in the Subandean belt during the last 2 m.y. have ranged between 8 and 11 mm/yr. Global positioning system stations at the back end of the Subandean belt at Tarija and Sucre display velocities of 8–12 mm/yr to the east with respect to a fixed South American reference frame (Bevis et al., 2001). This figure is in remarkably good agreement with the geologically determined rates over the last 2 m.y.

IMPLICATIONS TO PETROLEUM GEOLOGY

The Devonian source rocks, buried by thick Neogene foreland basin deposits and further loaded by the thrusting itself, entered the oil window contemporaneously with the deformation (Dunn et al., 1995). Some hydrocarbon generation in the Devonian source rocks could have started earlier, during the Mesozoic or even late Paleozoic (Moretti et al., 1996; Di Salvo and Villar, 1999; Starck, 1999), although the generation climax, expulsion, and migration are related to the Neogene tectonics. Cobbold (1999) proposed that the hydrocarbon generation might have produced an increase in the pore-fluid pressure, triggering the intermediate detachment in the source rocks because of a drop in the frictional resistance. The thrust front may follow the hydrocarbon maturation front, with ages of oil generation and migration getting younger to the east. Assuming a generation-expulsion depth of about 4 km (Reynolds et al., 2001), the base of the Devonian source rocks probably attained those depths at about 7 Ma at the western portion of the Subandean thrust belt, migrating to the eastern San Antonio, Aguaragüe, Duran-Madrejones, and Ipaguazu ranges at ages younger than 4 Ma. The relatively high rates of ongoing sedimentation and deformation indicated by both proposed models, together with the presence of high-pressure horizons in the source rocks at the intermediate structural level (Aramayo Flores, 1999), are in accordance with still-active hydrocarbon generation and migration. The proposed ages of hydrocarbon generation and migration are contemporaneous with those of deformation and anticlinal uplift, thus enhancing the possibilities of hydrocarbon entrapment in the Subandean ranges.

CONCLUSIONS

The Subandean ranges of northwestern Argentina comprise part of the foreland thrust and fold belt of the Andean orogen. Their principal characteristics include a thin-skinned deformation style and eastward vergence. Two major detachment levels are recognized: the basal one in the Silurian shales and a higher one in the Devonian shales. However, in the western part of this geologic province, where the intermediate structural level is reduced because of erosion, only the basal detachment level is present. As a result, a uniform mechanical behavior of the entire stratigraphic column can be observed in the Cinco Picachos and El Pescado ranges. Farther east, the Devonian shales thicken and become an important zone of decoupling.

Evolutionary stages of development of the belt are preserved in both east-west sections and locally along strike from south to north (e.g., at the Aguaragüe range). Such sections show that with increasing shortening, the degree of lift-off at the intermediate structural level also increased. The final geometries in the lower structural level are fault-bend folds with wide crests, steep front limbs and gentle backlimbs, whereas in the upper structural level above the zone of decoupling, both limbs are steep with box-fold geometries.

Our study provides the most detailed resolution yet on the ages of deformation anywhere in the Subandean belt. Two episodes are recognized. During the older episode, in-sequence deformation started in the west between 9 and 8.5 Ma and gradually propagated eastward, ending at about 1.2 Ma with the Aguaragüe range uplift. The younger deformation stage corresponds to an out-of-sequence movement, ranging from about 4.5 Ma to the present (Figure 12), with its age of initiation becoming younger to the east. The out-of-sequence movement started with the El Pescado fault reactivation, probably at about 4.5 Ma, and then migrated eastward with time.

The accurate age constraints on the thrusting also allow us to identify periods with simultaneous movements of different sheets. Best documented is the case of the Pintascayo and Baja Orán thrusts, where vertical separation diagrams suggest simultaneous motion between 6.9 and at least 4.7 Ma. Additionally, there has probably been young simultaneous and out-of-sequence motion on most of the thrust plates since 2 Ma.

Finally, we have been able to identify end-member shortening rate models based on assumptions of minimum and maximum duration of thrusting. The former case results in a model of two discrete periods of rapid shortening in the late Miocene and in the Quaternary, separated by a time of modest shortening during the Pliocene. The maximum-duration model suggests progressively increasing rates of shortening since 8 Ma. Both models suggest that Quaternary horizontal shortening rates are between 8 and 11 mm/yr, a figure that coincides well with global positioning system results from the area.

Our study has demonstrated how good age constraints are vitally important for understanding the evolution of a thrust belt, as well as for evaluating its hydrocarbon potential. Cenozoic strata have traditionally been ignored during exploration in the Subandean belt because the primary objectives are commonly the Devonian section. However, it is the Cenozoic that contains the record of thrust movement and anticlinal closure, as well as controlling the thermal history of the source and reservoir by burial depth.

REFERENCES CITED

Albariño, L., A. Dalenz Farjat, L. Alvarez, R. Hernández, and M. Pérez Leyton, 2002, Las secuencias sedimentarias del Devónico en el subandino sur y el Chaco. Bolivia y Argentina (CD-ROM): V Congreso de Exploración y Desarrollo de Hidrocarburos, Mar del Plata, Argentina: Instituto Argentino del Petróleo y del Gas, 21 p.

Allmendinger, R. W., 1998, Inverse and forward numerical modeling of Trishear fault-propagation folds: Tectonics, v. 17, p. 640–656.

Allmendinger, R. W., and T. R. Zapata, 2000, The footwall ramp of the Subandean decollement, northernmost Argentina, from extended correlation of seismic reflection data: Tectonophysics, v. 321, p. 37–55.

Anadón, P., L. Cabrera, F. Colombo, M. Marzo, and O. Riba, 1986, Syntectonic intraformational unconformities in alluvial fan deposits, eastern Ebro Basin margins (NE Spain), *in* P. A. Allen and P. Homewood, eds., Foreland basins: International Association of Sedimentologists Special Publication 8, p. 259–271.

Aramayo Flores, F., 1989, El cinturón plegado y sobrecorrido del norte argentino: Boletín de Informaciones Petroleras, Tercera Epoca, v. 17, p. 2–16.

Aramayo Flores, F., 1999, Estructura de las Sierras Subandinas del noroeste Argentino, *in* G. Gonzalez Bonorino, R. Omarini, and J. Viramonte, eds., Geología del Noroeste Argentino: Salta, Relatorio XIV Congreso Geológico Argentino, v. I: Asociación Geológica Argentina, p. 401–414.

Baby, P., G. Herail, R. Salinas, and T. Sempere, 1992, Geometry and kinematic evolution of passive roof duplexes deduced from section balancing: example from de Foreland thrust system of the southern Bolivia Subandean zone: Tectonics, v. 11, p. 523–536.

Belotti, H. J., L. L. Saccavino, and G. A. Schachner, 1995, Structural styles and petroleum occurence in the Subandean fold and thrust belt of northern Argentina, *in* A. J. Tankard, R. Suarez Soruco, and H. J. Welsink, eds., Petroleum basins of South America: AAPG Memoir 62, p. 545–555.

Bevis, M., E. Kendrick, R. Smalley Jr., B. Brooks, R. Allmendinger,

and B. Isacks, 2001, On the strength of interplate coupling and the rate of backarc convergence in the central Andes: an analysis of the interseismic velocity field: Geochemistry Geophysics Geosystems, v. 2, paper no. 2001GC000198.
Bilodeau, W. L., and T. C. Blair, 1986, Tectonics and sedimentation: timing of tectonics events using sedimentary rocks and facies: Geological Society of America Abstracts with Programs 18, p. 542.
Bischke, R. E., 1994, Interpreting sedimentary growth structures from well log and seismic data (with examples): AAPG Bulletin, v. 78, p. 873–892.
Cande, S. C., and D. V. Kent, 1995, Revised calibration of the magnetic polarity timescale for the late Cretaceous and Cenozoic: Journal of Geophysical Research, v. 100, p. 6093–6095.
Cobbold, P. R., 1999, Hydrocarbon generation, fluid overpressure and source rock detachments in thrust belts (abs.): Thrust Tectonic Conference, Royal Holloway, University of London, England. Session 2 Geodymanics of Thrust Systems, paper 4, p. 7–9.
Coira, B., and P. Caffe, 1999, Volcanismo Cenozoico de Puna norte, *in* G. Gonzalez Bonorino, R. Omarini, and J. Viramonte, eds., Geología del Noroeste Argentino: Salta, Relatorio XIV Congreso Geológico Argentino, v. I: Asociación Geológica Argentina, p. 371–386.
Coudert, L., M. Frappa, C. Viguier, and R. Arias, 1995, Tectonic subsidence and crustal flexure in the Neogene Chaco basin of Bolivia: Tectonophysics, v. 243, p. 277–292.
Cruz, C. E., L. M. Albariño, C. A. Sylwan, and H. J. Villar, 2001, Source rocks and hydrocarbons south of the Santa Cruz elbow, Bolivia and northwestern Argentina (abs.): AAPG Annual Convention, Official Program Book, Denver, Colorado, v. 10, p. A45.
Di Salvo, A., and H. J. Villar, 1999, Los sistemas petrolíferos del área oriental de la Cuenca Paleozoica Noroeste, Argentina: IV Congreso de Exploración y desarrollo de hidrocarburos Acta, Mar del Plata, Argentina: Instituto Argentino del Petróleo y del Gas, p. 83–100.
Dunn, J. F., K. G. Hartshorn, and P. W. Hartshorn, 1995, Structural styles and hydrocarbon potential of the Sub-Andean thrust belt of southern Bolivia., *in* A. J. Tankard, R. Suárez Soruco, and H. J. Welsink, eds., Petroleum basins of South America: AAPG Memoir 62, p. 523–453.
Echavarria, L. E., and R. W. Allmendinger, 2002, Diagramas de separación vertical, una herramienta para reconocer estratos de crecimiento: XV Congreso Geológico Argentino, El Calafate, CD-ROM, paper no. 391, 4 p.
Flemings, P. B., and T. E. Jordan, 1990, Stratigraphic modeling of foreland basins: interpreting thrust deformation and lithospheric rheology: Geology, v. 18, p. 430–435.
Giraudo, R., R. Limachi, E. Requena, and H. Guerra, 1999, Geología estructural de las regiones subandina y de piedemonte entre los 18° y 22°30′ lat. Sur, Bolivia. Un nuevo modelo de deformación: IV Congreso de Exploración y desarrollo de hidrocarburos Acta, Mar del Plata, Argentina, v. I: Instituto Argentino del Petróleo y del Gas, p. 405–426.
Gubbels, T. L., B. L. Isacks, and E. Farrar, 1993, High-level surfaces, plateau uplift, and foreland development, Bolivian central Andes: Geology, v. 21, p. 695–698.
Hardy, S., J. Poblet, K. McClay, and D. Waltham, 1996, Mathematical modelling of growth strata associated with fault-related fold structures, *in* P. G. Buchanan and D. A. Nieuwland, eds., Modern developments in structural interpretation, validation and modeling: Geological Society (London), p. 265–282.
Heller, P. L., N. S. Winslow, and C. Paola, 1986, Sedimentation and subsidence across a foreland basin, observations and results from the Western Interior (abs.): Geological Society of America Abstracts with Programs, v. 18, p. 634.
Hernández, R. M., J. Reynolds, and A. Di Salvo, 1996, Análisis tectosedimentario y ubicación geocronológica del Grupo Orán en el río Iruya: Boletín de Informaciones Petroleras, Tercera Epoca, v. 45, p. 80–93.
Hernández, R. M., C. I. Galli, and J. Reynolds, 1999, Estratigrafía del Terciario en el noroeste Argentino, *in* G. Gonzalez Bonorino, R. Omarini, and J. Viramonte, eds., Geología del Noroeste Argentino: Salta, Relatorio XIV Congreso Geológico Argentino, v. I: Asociación Geológica Argentina, p. 316–328.
Isaacson, P. E., and E. Diaz Martinez, 1995, Evidence for a middle–late Paleozoic foreland basin and significant paleolatitudinal shift, central Andes, *in* A. J. Tankard, R. Suarez Soruco, and J. Welsink, eds., Petroleum basins of South America: AAPG Memoir 62, p. 231–249.
Isacks, B. L., 1988, Uplift of the Central Andean Plateau and bending of the Bolivian orocline: Journal of Geophysical Research, B, Solid Earth and Planets, v. 93, p. 3211–3231.
Johnson, N. M., J. Stix, L. Tauxe, P. J. Severny, and R. A. K. Tahirkheli, 1985, Paleomagnetic chronology, fluvial processes and tectonic implications of the Siwalik deposits, near Chinji Village, Pakistan: Journal Geology, v. 93, p. 27–40.
Johnson, N. M., T. E. Jordan, P. A. Johnsson, and C. W. Naeser, 1986, Magnetic polarity stratigraphy, age and tectonics setting of fluvial sediments in an eastern Andean foreland basin, San Juan province, Argentina, *in* P. Allen and P. Homewood, eds., Foreland basins: International Association Sedimentologists Special Publication 8, p. 63–75.
Jordan, T. E., 1995, Retroarc foreland and related basins, *in* C. J. Busby and R. V. Ingersoll, eds., Tectonics of sedimentary basins: Cambridge, Massachussetts, Blackwell Science, p. 331–362.
Jordan, T. E., and R. N. Alonso, 1987, Cenozoic stratigraphy and basins tectonics of the Andes mountains, 20°–28° south latitude: AAPG Bulletin, v. 71, p. 49–74.
Jordan, T. E., P. B. Flemings, and J. A. Beer, 1988, Dating of thrust-fault activity by use of foreland basin strata, *in* K. L. Kleinspehn and C. Paola, eds., New perspectives in basin analysis: New York, Springer-Verlag, p. 307–330.
Jordan, T. E., R. W. Allmendinger, J. F. Damanti, and R. E. Drake, 1993, Chronology of motion in a complete thrust belt: the Precordillera, 30°–31°, Andes mountains: Journal of Geology, v. 101, p. 135–156.
Kley, J., 1998, Variable foreland shortening along the central Andes (15°–42° S): correlation with crustal thickness, lithospheric structure and the geometry of the Nazca Plate: X Congreso Latinoamericano de Geologia Acta, Buenos Aires, Argentina, v. II: Servicio Geológico Minero Argentino, p. 88–93.
Kley, J., and C. R. Monaldi, 1999, Estructura de las Sierras Subandinas y del Sistema de Santa Bárbara, *in* G. Gonzalez Bonorino, R. Omarini, and J. Viramonte, eds., Geología del Noroeste Argentino: Salta, Relatorio XIV Congreso Geológico Argentino, v. I: Asociación Geológica Argentina, p. 415–425.
Kley, J., J. Muller, S. Tawackoli, V. Jacobhsagen, and E. Manutsoglu, 1997, Pre-Andean and Andean-age deformation in the eastern Cordillera of southern Bolivia: Journal of South American Earth Science, v. 10, p. 1–19.
Leturmy, P., J. L. Mugnier, P. Vinour, P. Baby, B. Colletta, and E. Chabron, 2000, Piggyback basin development above a thin-skinned thrust belt with two detachment levels as a function of interactions between tectonic and superficial mass transfer: the case of the Subandean zone (Bolivia): Tectonophysics, v. 320, p. 45–67.
Marshall, L., T. Sempere, and M. Gayet, 1993, The Petaca (late Oligocene–middle Miocene) and Yecua (late Miocene) formations of the Subandean-Chaco basin, Bolivia, and their

tectonic significance: Documents Laboratoire Geologique Lyon, v. 125, p. 291–301.
Medwedeff, D. A., 1989, Growth fault-bend folding at southeast Lost Hills, San Joaquin Valley, California: AAPG Bulletin, v. 73, p. 54–67.
Medwedeff, D. A., and J. Suppe, 1986, Growth fault-bend folding precise determination of kinematics, timing and rates of folding and faulting from syntectonic sediments (abs.): Geological Society of America Abstracts with Programs, v. 18, p. 692.
Mingramm, A., A. Russo, A. Pozzo, and L. Cazau, 1979, Sierras Subandinas, *in* J. C. M. Turner, ed., Geología Regional Argentina: Cordoba, Academia Nacional de Ciencias, v. 1, p. 95–138.
Mombru, C. F., and F. Aramayo Flores, 1986, Geología del Yacimiento de Aguaragüe: Boletín de Informaciones Petroleras, Tercera Epoca, v. 6, p. 53–64.
Moretti, I., P. Baby, E. Mendez, and D. Zubieta, 1996, Hydrocarbon generation in relation to thrusting in the Sub-Andean zone from 18° to 22° S, Bolivia: Petroleum Geoscience, v. 2, p. 17–28.
Mosquera, A., 1999, Evolución temporal de la deformación en las Sierras Subandinas Orientales: IV Congreso de Exploración y desarrollo de hidrocarburos Acta, Mar del Plata, Argentina: Instituto Argentino del Petróleo y del Gas, p. 563–578.
Ramos, V. A., and R. N. Alonso, 1995, El mar Paranense en la provincia de Jujuy: Revista del Instituto de Geología y Minería, Jujuy, Argentina, v. 10, p. 73–82.
Rasanen, M. E., A. M. Linna, J. C. R. Santos, and F. R. Negri, 1995, Late Miocene tidal deposits in the Amazonian foreland basin: Science, v. 269, p. 386–390.
Raynolds, R. G. H., and G. D. Johnson, 1985, Rates of Neogene depositional and deformational processes, northwest Himalayan foredeep margin, Pakistan, *in* N. J. Snelling, ed., The chronology of the geological record: Oxford, Blackwell, Geological Society Memoir 10, p. 297–311.
Reynolds, J. H., C. I. Galli, R. M. Hernández, B. D. Idleman, J. M. Kotila, R. V. Hilliard, and C. W. Naeser, 2000, Middle Miocene tectonic development of the transition zone, Salta Province, northwest Argentina: magnetic stratigraphy from the Metán Subgroup, Sierra de González: Geological Society of America Bulletin, v. 112, p. 1736–1751.
Reynolds, J. H., R. M. Hernández, C. I. Galli, and B. D. Idleman, 2001, Magnetostratigraphy of the Quebrada La Porcelana section, Sierra de Ramos, Salta Province, Argentina: initial age limits on the regional Neogene lithostratigraphy and uplift of the southern Sierras Subandinas: Journal of South American Earth Sciences, v. 14, p. 681–692.
Schmitz, M., and J. Kley, 1997, The geometry of the Central Andean backarc crust: joint interpretation of cross-section balancing and seismic refraction data: Journal of South American Earth Sciences, v. 10, p. 99–110.
Sempere, T., 1995, Phanerozoic evolution of Bolivia and adjacent regions, *in* A. J. Tankard, R. Suarez Soruco, and H. J. Welsink, eds., Petroleum basins of South America: AAPG Memoir 62, p. 207–230.
Sempere, T., G. Erial, J. Oller, and M. Bonhomme, 1990, Late Oligocene–early Miocene major tectonics crisis and related basins in Bolivia: Geology, v. 18, p. 946–949.
Sempere, T., E. Aguilera, J. Doubinger, P. Janvier, J. Lobo, J. Oller, and S. Wenz, 1992, La Formation de Vitiacua (Permien Moyen a superieur Trias? Inferieur, Bolivie du sud): stratigraphy, palynologie et paleontology: Neues Jahrbuch fuer Geologie and Palaeontologie Abhandlungen, v. 185, p. 239–253.
Starck, D., 1995, Silurian–Jurassic stratigraphy and basin evolution of northwestern Argentina, *in* A. J. Tankard, R. Suarez Soruco, and H. J. Welsink, eds., Petroleum basins of South America: AAPG Memoir 62, p. 251–268.
Starck, D., 1999, Los sistemas petroleros de la Cuenca de Tarija: IV Congreso de Exploración y desarrollo de hidrocarburos Acta, Mar del Plata, Argentina: Instituto Argentino del Petróleo y del Gas, p. 63–82.
Starck, D., and A. Schulz, 1996, La configuración estructural del límite entre Cordillera Oriental y Sierras Subandinas en el extremo norte de la Republica Argentina: Boletín de Informaciones Petroleras, Tercera Epoca, v. 52, p. 39–46.
Starck, D., E. Gallardo, and A. Schulz, 1992, La Cuenca de Tarija: estratigrafía de la porción Argentina: Boletín de Informaciones Petroleras, Tercera Epoca, v. 30, p. 2–14.
Steidtmann, J. R., and J. F. Schmitt, 1988, Provenance and dispersal of tectonics sediments in thin-skinned, thrust terrains, *in* K. L. Kleinspehn and C. Paola, eds., New perspectives in basin analysis: New York, Springer-Verlag, p. 353–356.
Suppe, J., G. Chou, and S. Hook, 1992, Rates of folding and faulting determined from growth strata, *in* K. R. McClay, ed., Thrusts tectonics: London, United Kingdom, Chapman & Hall, p. 105–121.
Viramonte, J. G., J. H. Reynolds, C. Del Papa, and A. Disalvo, 1994, The Corte Blanco granatiferous tuff: a distinctive late Miocene marker bed in northwestern Argentina applied to magnetic polarity stratigraphy in the Rio Yacones, Salta Province: Earth and Planetary Science Letters, v. 121, p. 519–531.
Vistalli, M. C., 1999, Cuenca Siluro Devonica, *in* G. Gonzalez Bonorino, R. Omarini, and J. Viramonte, eds., Geología del noroeste Argentino: Salta, Relatorio XIV Congreso Geológico Argentino, v. I: Asociación Geológica Argentina, p. 168–184.
Wiltschko, D. V., and J. A. Dorr, 1983, Timing of deformation in overthrust belt and foreland of Idaho, Wyoming and Utah: AAPG Bulletin, v. 67, p. 1304–1322.
Zehnder, A. T., and R. W. Allmendinger, 2000, Velocity field for the Trishear model: Journal of Structural Geology, v. 22, p. 1009–1014.